01 May 2012

Scaling Relations and the Role of Bond-Charge to the Electron Transmission through Two Coupled Aharonov-Bohm Rings

Cheng-Hsiao Wu
Missouri University of Science and Technology, chw@mst.edu

Lam C. Tran

C. A. Cain

Recommended Citation

C. Wu et al., "Scaling Relations and the Role of Bond-Charge to the Electron Transmission through Two Coupled Aharonov-Bohm Rings," *Journal of Applied Physics*, vol. 111, no. 9, American Institute of Physics (AIP), May 2012.
The definitive version is available at https://doi.org/10.1063/1.4705513

Scaling relations and the role of bond-charge to the electron transmission through two coupled Aharonov-Bohm rings

C. H. Wu, L. Tran, and C. A. Cain
Department of Electrical and Computer Engineering, Missouri University of Science and Technology, 301 W 16th St., Rolla, Missouri 65409, USA

(Received 28 October 2011; accepted 23 March 2012; published online 4 May 2012)

Electron transport and the exact scaling relations for two irreducibly coupled Aharonov-Bohm (AB) rings with two external terminals attached are investigated. In coupled AB rings, a center common path exists where the phase of the electron wave function can be modulated by two applied fluxes simultaneously. The two coupled rings can be considered as two coupled atoms where Fermi level crossings exist not only between bonding states but also between bonding and anti-bonding states when the applied flux is varied in one of the two cases studied. We show that when the smallest atomic-sized coupled rings are scaled up any odd number of times, an identical electron transmission is preserved. When two terminals are attached to isolated coupled AB rings, there is a further redistribution of bond-charge stored within the center common path. The shift of the electron charge distribution to favor one end of the common path is accompanied by the redistribution of the two partial waves that traverse through the two arms from the input to the output terminal. The flux can control which arm the electron traverses through more favorably, and hence, the center path behaves like a flux-controlled charge reservoir for the electron transport. The unbalanced charge in the entire structure creates a space-charge effect much like a p-n junction. The paradox of the delocalization of the electron wave when two AB rings are coupled and the subsequent localization effect of the electron transport in a quantum network are described.
 [http://dx.doi.org/10.1063/1.4705513]

I. INTRODUCTION

In the mesoscopic and microscopic world, it can be useful to investigate strictly one-dimensional networks in order to gain physical insights. An Aharonov-Bohm (AB) ring of this size with two terminals was first investigated experimentally over two decades ago and the effect has since been studied extensively.[1–8] While there are several allowed one-dimensional paths that can be embedded into a mesoscopic ring of small cross section, it has been calculated and experimentally shown that only one dominant path will persist.[9–15] The behavior of this dominant class is of key interest. There are similarities between classical waveguides and the electron waveguides presented here in a two-terminal AB ring. In a rectangular waveguide (in the microwave region) with cross-sectional dimensions a and b, there are two distinctive classes of propagation, transverse electric (TE_{mn}) and transverse magnetic (TM_{mn}), described by zero electric and magnetic fields in the direction of wave vector $\vec{k}$, respectively. Each propagation mode (mn) within the TE or TM class is then determined by how many half-integer wavelengths can fit within the cross section. The higher divisions are the high-frequency modes while the lowest division (fundamental mode) is simply a and b. In the corresponding electron waveguide situation, this is reversed. The minimum division of an AB ring is the atomic spacing, with the lowest-order mode corresponding to an atomic-sized ring. In principle, rings of a higher-order can exist in a larger structure, such as in carbon nanotubes or graphene lattice structures.[16,17] Mesoscopic rings will possess small cross-sectional areas consisting of several embedded one-dimensional rings. This raises an important question of the scaling relations between the lowest division AB ring and its higher-order counterparts. In a one-dimensional AB ring, the total number of atoms, M, is large but finite. Even when the value of M is approaches very large values, it is not valid to assume the $M \rightarrow \infty$ limit. This is because three distinctive classes of propagation exist, much like the TE and TM classes in microwaves. It has been shown[18] that the value of M is one of the determining parameters for this classification. In strictly one-dimensional rings with two terminals, the total number of atoms is denoted by $M = m + n$, where m is the number of atoms in the upper arm, while n is the corresponding number in the lower arm. In Class I, m and n are both even numbers. Class II is when m and n are both odd, making M even. Lastly, Class III is when M is odd, which constricts m and n to differ in parity. The asymmetrical result is that the upper arm and the lower arm must differ by at least one atomic spacing and hence, the flux periodicity is doubled at $(\Phi_0/_2)$. This is the universal double periodicity for any combination of an odd-numbered ring.[18] The important result is that this finiteness prevents one from treating the network as a continuum. Therefore, a mesoscopic ring consists of 1D rings, which propagate like a TE_{mn} or TM_{mn} class at a high-frequency mode or at a higher-order division of the length a or b. To demonstrate a lower-order mode, an AB ring has to be reduced in atomic size and hence, there must be fewer embedded one-dimensional rings. In this case, three distinctive classes of AB rings can be exhibited separately. At a low-order propagation mode, an AB ring appears as a 1D atomic-sized ring with small M, while at a higher-order mode, a collection of integrated one-dimensional rings.

When M is monotonically increased the electron transport cycles through three different classes of propagation or three different transmissions and two flux periodicities, and hence uniquely distinguishes mesoscopic from macroscopic systems. Scaling relations exist, which demonstrate a preservation of transmission behavior within each class if the value of M (m,n) is scaled up properly. The scaling relations for simple two-terminal rings will be briefly revisited first before we present relations for coupled AB rings.

Earlier investigations by one of us has shown[18] that the electron transmission through a two-terminal AB ring is physically equivalent to a chain of flux-assisted harmonic oscillators of the same topology (see Fig. 2 in Ref. 21) when subjected to an external perturbation by using a set of linear node equations described in Sec. II. Therefore, intuitively, it is very easy to visualize that a four-atom AB ring ($M=4$) can have equal arm lengths (two atomic spacings) between the input to the output terminals. At zero flux, the two partial waves scattered at the input will arrive at the output in phase, resulting in total transmission. However, at the flux value of $\Phi = \pm(\Phi_0/_2)$, where Φ_0 is the elementary flux quanta hc/e, the two partial waves will arrive with a phase difference $|\delta| = \pi$, resulting in a total reflection. If the number of atoms were doubled ($M=8$), phase conditions will remain the same. The harmonic oscillators are topologically equivalent in both cases (the scaling relation), hence the flux dependence of the electron transmission from zero at $\Phi = \pm(\Phi_0/_2)$ to 1 at $\Phi = 0$ remains unchanged. The governing set of equations for the network are unchanged except the atomic spacing a is changed to $2a$ in all the $\cos(ka)$ terms (the $M\beta$ term in Eq. (36) of Ref. 18 is an invariant quantity). Thus, an $M =$ 400 AB ring with $m = n = 200$ corresponds to an arbitrary higher-order mode of Class I, whose fundamental mode is given by $M = 4$ $(m = n = 2)$. The importance consequence of this argument is that there is no need to investigate the electron transmission through a large structure. An equivalent small-scale toy model, corresponding to the fundamental propagation mode, is sufficient due to the manifestation of the scaling relations.

In this paper, we investigate the electron transmission through two irreducibly coupled AB rings in terms of the added scaling relations (Sec. III) and the important role played by the bond-charge storage behavior within the center common path (Sec. IV). An isolated AB ring can be considered a man-made atom with a circulating persistent current playing the role of the orbiting electron, except the positive charge is uniformly distributed in the ring. When two AB rings are irreducibly coupled by a center common path, the situation is similar to that of two coupled atoms where bonding and anti-bonding effects are present.[19] The persistent currents are now controlled by the two external fluxes Φ_1 and Φ_2. The clockwise (counter-clockwise) persistent current is analogous to spin-up (spin-down) states, so that computing networks comprised of AB rings can be described in a similar manner as spintronics.[20] Therefore, correlating the charge storage behavior within the network to the electron transport is of significant interest. As we will show later, there is a charge redistribution along the center path that becomes asymmetrical when two terminals are attached as a result of the perturbation. Our investigation is motivated by the possible applications of using coupled AB rings for computing in place of two equivalent coupled spins.[21]

II. NODE EQUATION APPROACH

In our work, we used the quantum network approach developed earlier[18,21–24] to calculate the one-dimensional electron transport of a given network with elastic scatterings at the node points. A quantum network is composed of nodes and bond lengths that connect adjacent nodes. Within a bond, the Schrödinger equation is satisfied. Furthermore, at each node point, the Kirchhoff law for conservation of current must also hold.[25] The resulting linear set of node equations is an exact relationship between the electron wave function at a given node with all neighboring nodes. This is physically similar to a network of coupled harmonic oscillators of the same topology with masses and springs, except the value of the spring constant is flux-modulated. The equivalence this method compared to the traditional S-matrix approach has been established.[18] The set of node equations for a network can then be written as

$$\left[\sum_y \cot(kl_{xy}) - iD\right]\Psi(x) - \sum_y [\csc(kl_{xy})\exp[i\phi l_{xy}]\Psi(y)] = 0, \tag{1}$$

where $k = \sqrt{2mE/\hbar}$, and E is the electron energy. The phase modulation between atoms in the ring is defined as $\phi = (2\pi/M)(\Phi/\Phi_0)$. $\mathrm{D} = (1-\mathrm{R})/(1+\mathrm{R})$, where R is the reflection amplitude if node x is an input, $\mathrm{D} = -1$ if node x is an output, and $\mathrm{D} = 0$ otherwise. This set of node equations allows one to solve for all the electron wave functions at each node in the network and determine the transmission probabilities $T_{sum} = 1 - |R|^2$ if there are external terminals attached. The transmission probability is then used to calculate the conductance as described in the Landauer-Büttiker formalism.[26–31] Note that Eq. (1) is not a tight-binding approximation, but an exact solution.

III. SCALING RELATIONS FOR IRREDUCIBLY COUPLED AB RINGS

When two simple AB rings are merged together where they share a finite center common path,[16,19,21,24] they are referred to as irreducibly coupled. We examined two cases: a single bond and a double bond. In this configuration, the electron wave function along the center common path can be modulated by two fluxes Φ_1 and Φ_2. There are three primary classes of electron transmission: when the number of atoms in each ring of (I) are even, (II) odd, and (III) odd-even pairs.[21] We investigated the validity of extending the scaling relations from a simple ring to coupled AB rings. Two coupled rings can be generally described as (l,m,n), which defines the atomic spacings in the left ring, right ring, and center path, respectively. Starting with the smallest M3S AC case, where $(l,m,n) = (2,2,1)$ and M3 stands for a total of three atoms (the smallest odd number) in each ring coupled together by a single center path with terminals at A and C as shown in Fig. 1, we demonstrate that the transmission is

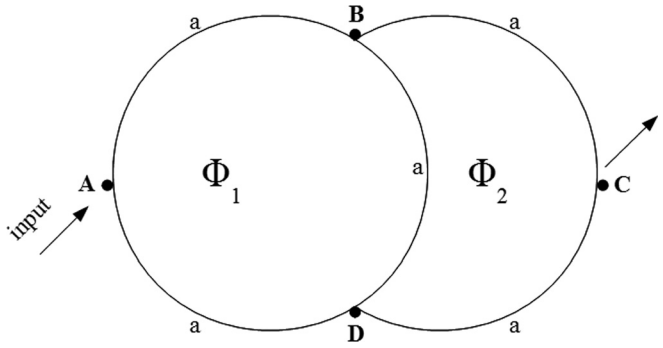

FIG. 1. M3S AC network where two odd $M = 3$ rings are coupled together. If a second center path was connected between B and D, then the network would be considered a double bond, denoted by M3D. The areas for each ring are implied to be equal.

exactly preserved when the network is scaled up by any odd n-factor, with a half-period flux shift depending if the particular scaled up rings are classified as $M = [5,9,13,17,21,\ldots,4N+1]$ or $M = [3,7,11,15,19,\ldots,4N+3]$. The results are shown in Fig. 2. There is a difference of a half-period flux shift between $M = 4N+1$ and $M = 4N+3$ in odd-numbered coupled rings which is not observed for a single odd ring. If a second center path is added to the M3S structure, the network now has a double bond and is denoted by M3D. This additional path does not alter the flux period or possible flux shift, but does affect the transmission.

The M4S AD network is shown in Fig. 3, where $(l,m,n) = (3,3,1)$. This is the smallest even coupled ring configuration. Like the M3 structure, a double bond M4D network can be created by simply inserting another common path into an M4S. The transmission behavior is again preserved in Fig. 4 when scaling by any odd n-factor of M4. While the M3 scaling cases exhibit a half-period flux shift, such a difference disappears in even networks, since the total atoms always remain within the same $M = [4,8,12,16,20,\ldots,4N]$ group, never crossing into $M = [6,10,14,18,22,\ldots,4N+2]$. The same would hold true if one were scaling a coupled network initially falling into the $4N+2$ group.

Combining these results with previous works, it can be sufficiently stated that a fixed quantum network can be scaled any odd number of times and exhibit identical

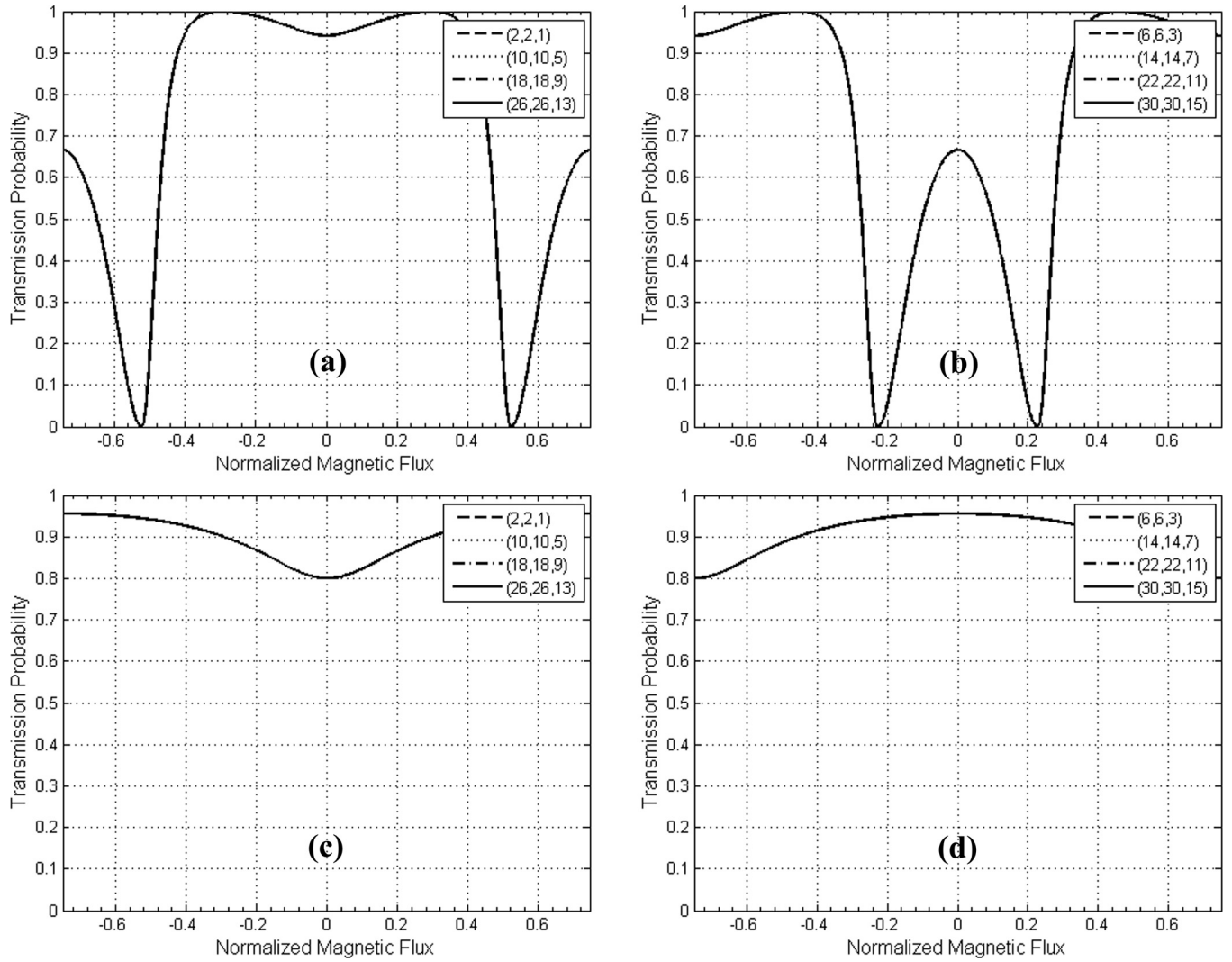

FIG. 2. Transmission results when the smallest (2,2,1) structure for M3S (a) and M3D (c) networks is scaled up by an odd n-factor leading to each ring having $M = [3,7,11,15,19,\ldots,4N+3]$ atoms. If the n-factor leads to $M = [5,9,13,17,21,\ldots,4N+1]$, then M3S is depicted by (b) and M3D by (d). Note the half-period flux shift of $(3/4)\Phi_0$ between the two classifications for both bonds.

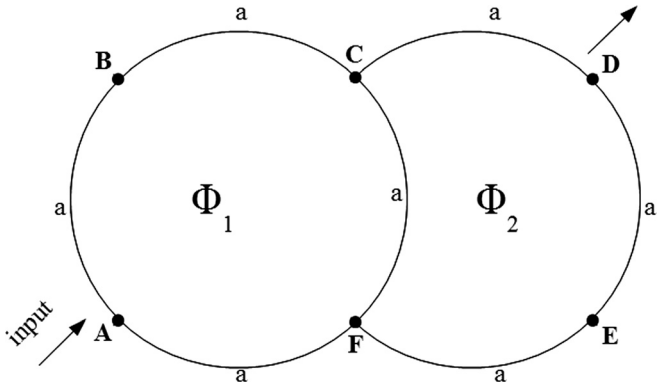

FIG. 3. M4S AD network where two even $M = 4$ rings are coupled together. If a second center path was connected between C and F, then the network would be considered a double bond, denoted M4D. The areas of each ring are implied to be equal.

transmission behavior, i.e., changing the atomic spacings in the network from (3,3,1) to (9,9,3) and so on has no effect on the transmission. These observations are very important because together they state that an atomic-scale network can be scaled-up to a mesoscopic size as long as the electron coherence is maintained. Since there are only three classes of coupled rings, the scaling relations imply that any fabricated mesoscopic structure of small cross section will exhibit the dominant electron transmission mode present in one of the three classes.

IV. CHARGE DISTRIBUTION AND ITS RELATION TO THE ELECTRON TRANSMISSION IN TWO COUPLED AB RINGS

In an isolated situation of two even coupled AB rings, the total amount of electron charge accumulated along the center common path can be varied by the applied fluxes Φ_1 and Φ_2 to reach a peak value or total depletion. In our study, we examine when fluxes $\Phi_1 = \Phi_2 = \Phi$ only. As the electron charge starts to be depleted with an increasing value of the applied flux Φ, the electron density is redistributed, so that the outer loop of the weakened bonding orbital get more share of the electron density as one expects. The corresponding electron density profiles are plotted in Figs. 5(a) and 5(b) for the entire flux period. The electron charge is integrated over the entire center path and then evaluated as a fraction of the total charge in the normalized unit of a single electron e, shown in Fig. 5(c). In the double bond situation, the electron charge is depleted monotonically as the flux increases due to the Fermi level residing at a bonding orbital over the entire flux period (Fig. 6(a)). The average charge at the center path over the entire flux period is calculated to be $0.2355e$ of the total charge in the entire structure, which is less than the value of $0.25e$ in the uniform charge distribution for two bonds out of the 8 total. However, for the single bond situation, the Fermi level of the coupled rings starts at an antibonding orbital, rather than a bonding orbital, with a small electron density along the center path at zero flux. There is then a Fermi level crossover to a lower energy bonding orbital at $\Phi = \pm(2/9)\Phi_0$ as the applied flux is increased where there is a sudden inrush of charge into the common path, as shown in Figs. 5(b)–5(d) and 6(b). The average electron charge for the single bond case is $0.1112e$ of the total charge. Again this value is less than one expects ($0.143e$) from a uniform charge distribution for one bond out of 7 total. The Fermi level crossing uniquely defines where uniform charge distribution takes place between all bonds in the network. The discontinuity in our calculations can be attributed to the charge instantly being depleted from a higher energy antibonding orbital to fill the lower bonding orbital at this Fermi level crossing. Note that right at the crossing, electron density will be adjusted to a uniform distribution first before any further changes. At flux values less than the crossing, there is no net current flowing through the center path, since there is no electron density at the midpoint. Once the Fermi level crosses into the bonding orbital, the net current remains zero, since the directional derivative of the electron density vanishes. It is obvious that whenever two AB rings are coupled,

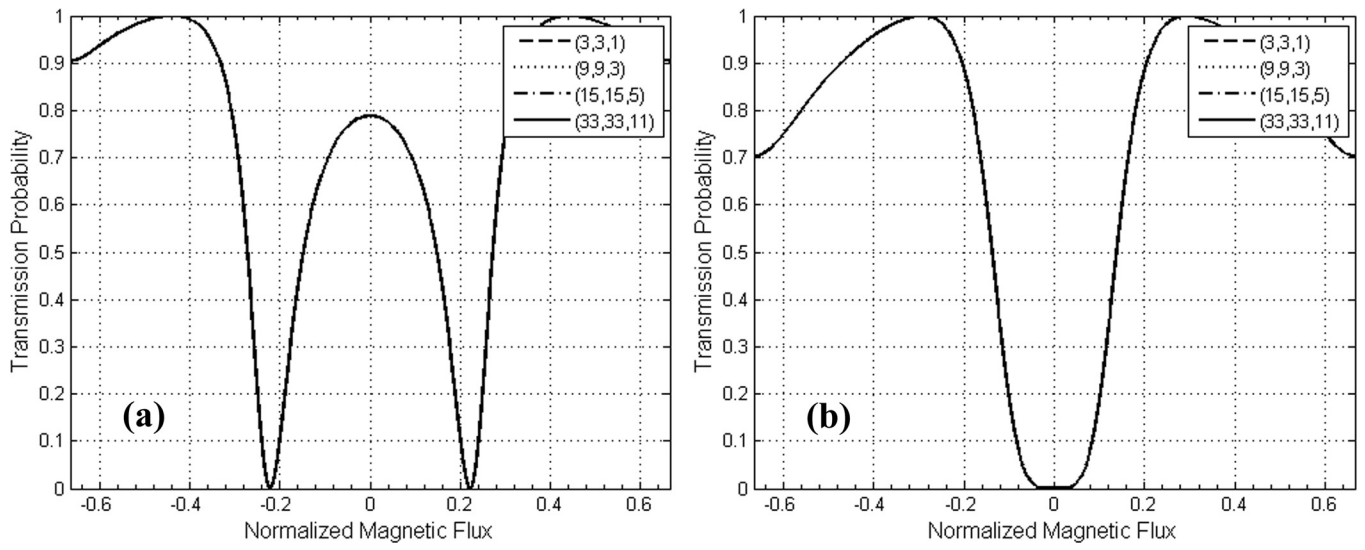

FIG. 4. Transmission results for M4S AD (a) and M4D AD (b) networks. The transmission remains exact for any odd n-factor, without a flux shift since all odd scaling configurations fall into the same 4N group.

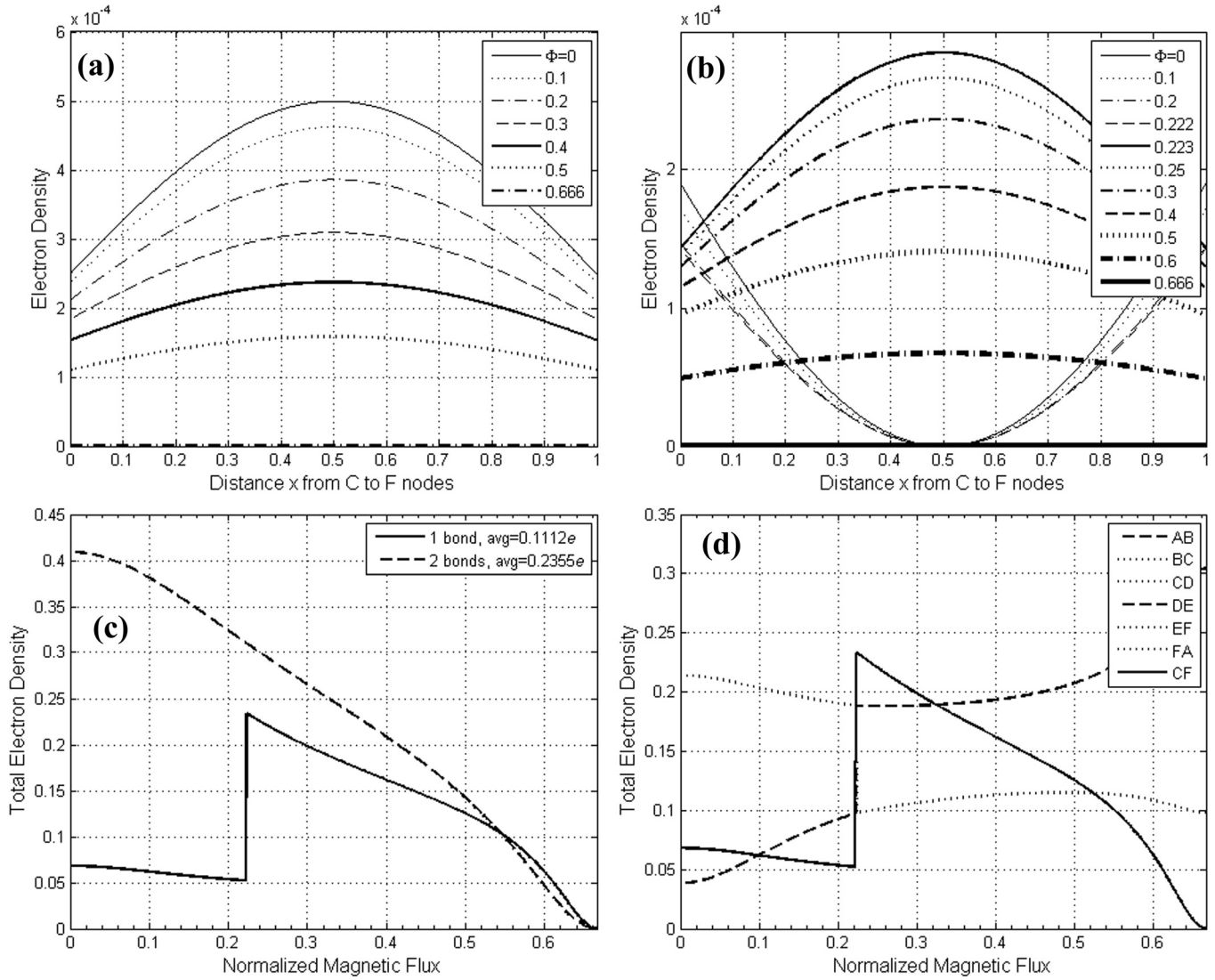

FIG. 5. Isolated M4D (a) and isolated M4S (b) common path densities. (c) Total density along common path. (d) Total density for all bonds in M4S network. At the Fermi level crossing, there is uniform distribution and is the cause of the discontinuity.

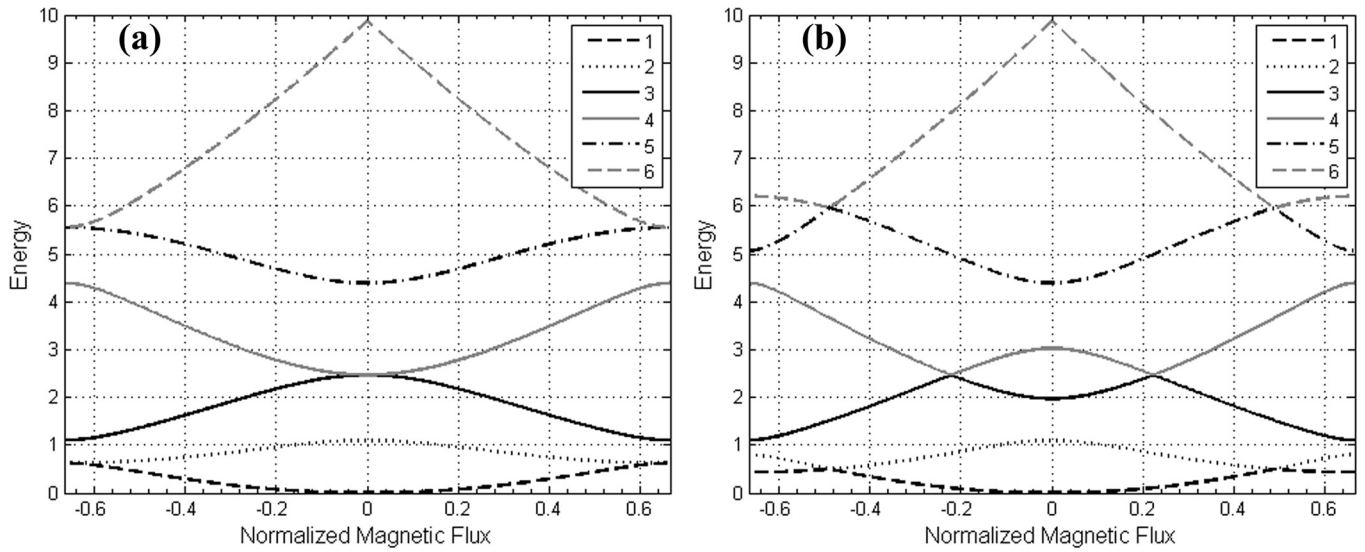

FIG. 6. (a) M4D and (b) M4S band structures, also shown as part of Fig. 4 in Ref. 21. The Fermi level for the M4S network encounters a crossover between an anti-bonding to bonding orbital, not present for M4D. Reprinted with permission from J. Appl. Phys. **110**, 054315 (2011). Copyright 2011 American Institute of Physics.

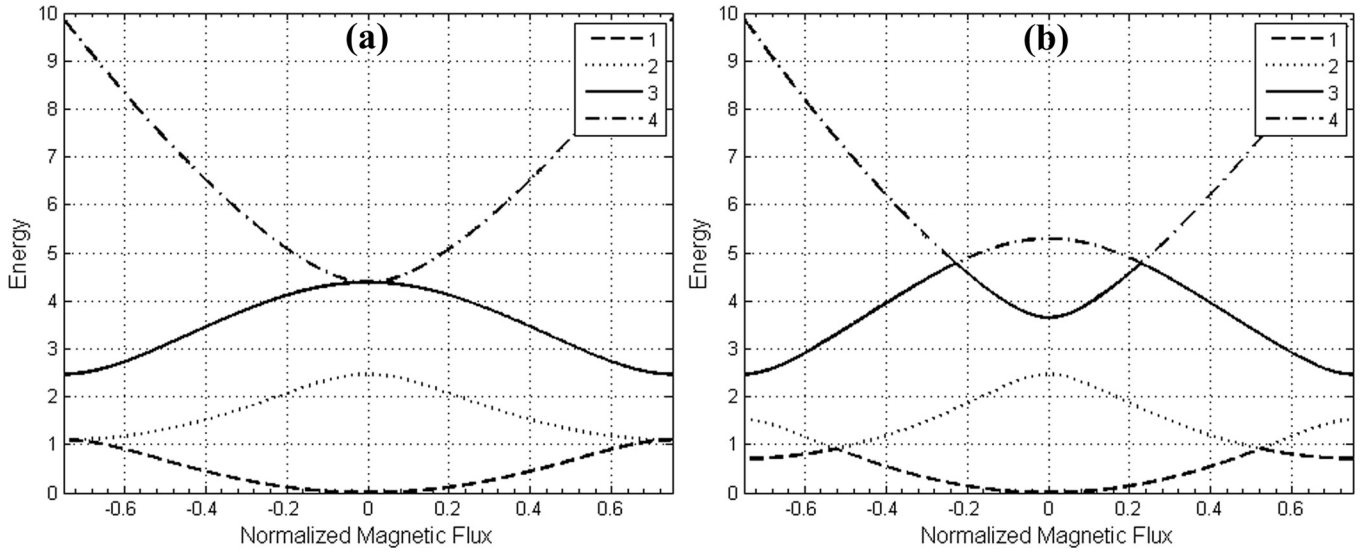

FIG. 7. M3D (a) and M3S (b) band structures. Note that the Fermi level for the M3S network encounters a crossover to a stronger bonding orbital, which is not present for M3D.

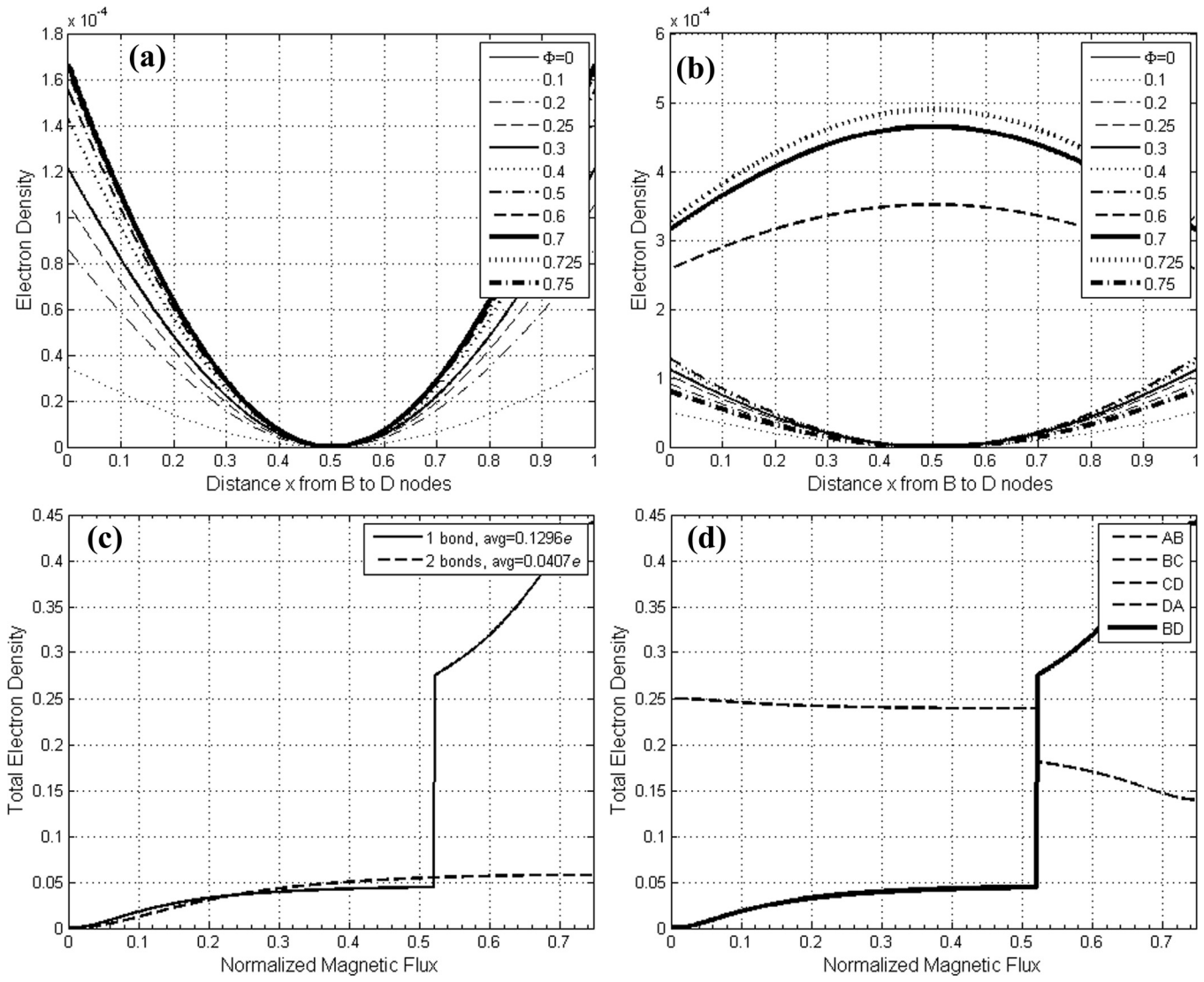

FIG. 8. Isolated M3D (a) and isolated M3S (b) common path densities. (c) Total density along common path. (d) Total density for all bonds in M3S network. A uniform distribution exists at the Fermi crossing, leading to the discontinuity.

there is an equilibrium redistribution of electron charge at the center common path, which can result in a fractional electron charge circulating around the larger outer loop. This space-charge effect is no different from bringing an n-type and a p-type semiconductor together to form a classical diode at equilibrium, except now the space-charge is from two metallic rings. This origin is of course from the delocalization tendency when two rings (two atoms) are coupled and the degree of which depends whether the Fermi level resides at a bonding or anti-bonding orbital.

There is an opposite effect in odd coupled AB rings. That is, as flux is increased, there is now a monotonic increase in charge accumulation along the common path. As in the transmission perspective, this fundamental difference in charge accumulation behavior between even and odd networks is very interesting. The M3S (single bond) network possesses a Fermi level crossing at $\Phi \approx \pm 0.522\Phi_0$ where a stronger bonding orbital is then encountered out to the zone boundary, as depicted in Fig. 7(b). The existence of this Fermi crossover can be further explained by the sudden burst of charge at the center common path, leading to the average charge of the single-bond to possess $0.1296e$, dominating the double bond network (lacking such a crossing), which only has an average of $0.0407e$. These results are shown in Fig. 8. At the Fermi level crossing for the M3S case, there is again a uniform charge distribution among all of the bonds in the network, even though this crossing is between two like (bonding) orbitals, unlike the M4S case discussed previously. The discontinuity in this region is again a signature of the Fermi level crossing.

We further examined the situation when two externals terminals are attached to even coupled rings and study the relation between the electron transport and the behavior of the electron density at the center common path. In Fig. 9, we show the corresponding electron densities of Fig. 5 when two terminals are attached at nodes A and D. There is now an asymmetry between the upper and lower branches of the ring. The two electron partial waves scattered at the input terminal A are unequal in amount and now favor passing more through node C and less through node F to arrive at the

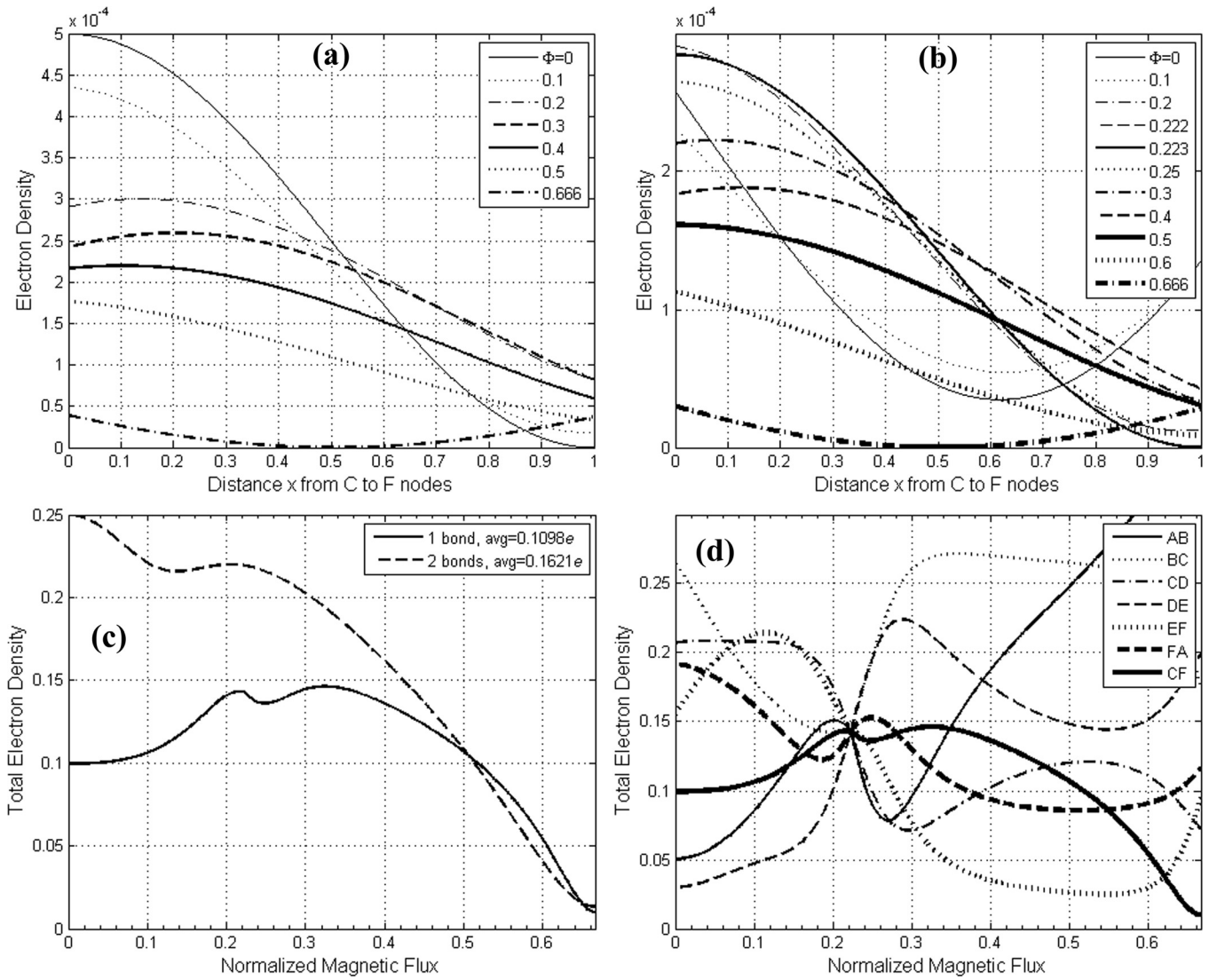

FIG. 9. M4D AD (a) and M4S AD (b) common path densities. (c) Total density along common path. (d) Total density for all bonds in M4S AD network. Note that while there are no electron density discontinuities at the Fermi crossing flux, the uniform density distribution is achieved at the crossing nonetheless.

output D. This bond charge redistribution within the common path is closely related to the electron transmission through the terminals. It implies that when two external terminals are attached the electron charge stored within the segment of the center path not only redistributes with the outer loop bonds but also redistributes within the path itself by shifting more of its share of the charge to one end (at node C) to accommodate the mode of the electron transport. There is always a tiny amount of residual charge remaining in the path for both double and single bond situations at the flux value of $\Phi = (2/3)\Phi_0$. Thus, whenever two external terminals are attached, the charge at the center common path cannot be totally emptied as in the case of isolated coupled rings if transmission is said to be possible. However, the total integrated charge along the common path is very similar to the situation of the two isolated coupled rings, even though at the zone boundary ($|\Phi| = (2/3)\Phi_0$), the total charge is not exactly zero, as shown in Fig. 9(c). As a result of this charge redistribution behavior, the incoming electron will favor passing through one of the two arms (nodes ABCD) by adjusting the amount of the two partial waves in each arm accordingly. This is in sharp contrast with the situation of having two equal partial waves in a simple even AB ring of two equal paths with no center common path. Thus, the network's classification determines which path the electron will prefer to take between source and drain. Those classes are determined by the parameters of (l,m,n) as discussed earlier in Sec. III. We note there is a similarity between the electron transport when the Fermi energy is at a bonding orbital at the range of $(2/9)\Phi_0 < |\Phi| < (2/3)\Phi_0$ for a single bond and $0 < |\Phi| < (2/3)\Phi_0$ for the double bond situation, both depicted previously in Fig. 4. For the anti-bonding orbital at $0 < |\Phi| < (2/9)\Phi_0$ in the single bond case, there is a drop in the electron density along the common path, thus an electron traverses through the coupled ring in that flux range as if the two nodes at the ends of the center common path are weak scattering centers and the transmission probability peak is reduced to 0.8 from 1 for a simple AB ring. When two terminals are attached, the charge density discontinuities at the Fermi crossing previously observed in the isolated network

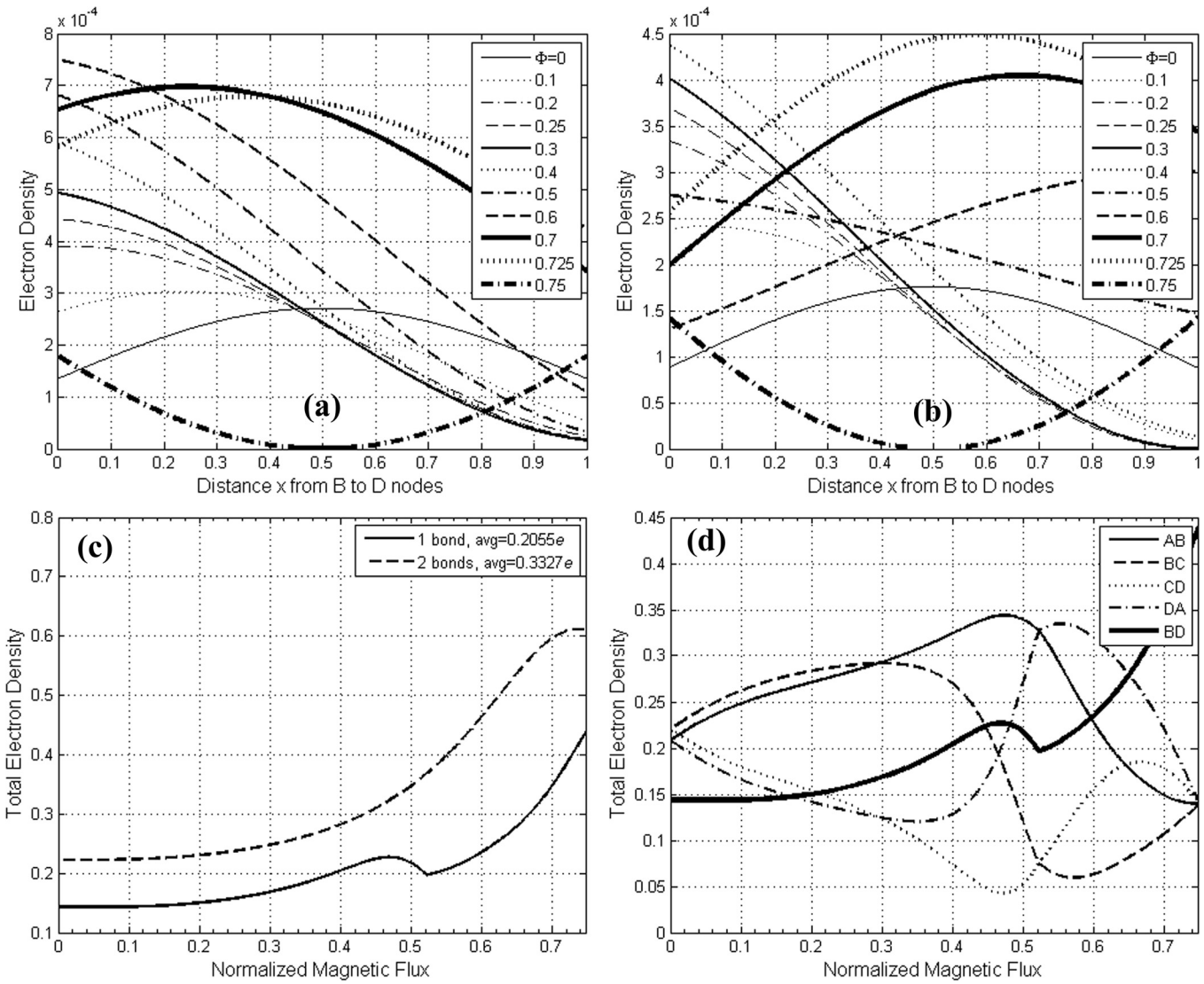

FIG. 10. M3D AC (a) and M3S AC (b) common path densities. (c) Total density at the common path. (d) Total density for all bonds in M3S AC network. Note that at the Fermi crossing, the uniform distribution that once existed in the isolated network is no longer present.

(Fig. 5) are removed by the perturbation and a more subtle change is observed due to the mode of transport now controlling how the charge is allocated within the bonds.

When two odd coupled rings have terminals attached at A and C, forming equal upper and lower arm lengths, a similar general trend of charge shifting to the upper end (at node B) of the common path is present, as shown in Fig. 10. The single bond structure, however, exhibits this behavior up to the Fermi level crossing to the lower (and hence stronger) bonding orbital, but the charge then shifts more to the lower end (at node D) of the common path past this point to the zone boundary. Since the terminal locations form a symmetric outer loop, there is a corresponding symmetrical charge distribution at the center common path for zero flux and at the zone boundary $|\Phi| = (3/4)\Phi_0$, which can be attributed to a singularity in transmission at this value. Unlike the isolated odd coupled rings, there is now a clear difference of additional total charge accumulation in the common path for a double bond, compared to a single bond. Even though in the isolated situation the single bond contained a Fermi level crossing to a stronger (lower) bonding orbital, the sudden burst of charge (at the discontinuity) for uniform distribution once present is now mitigated by the network having to accommodate the mode of transport for symmetric terminals. Thus, the double bond takes a greater share of the charge, with an average of about $0.3e$, compared to the single bond taking only about $0.2e$. Note how both are very close to uniform charge distributions of $^1/_3$ and $^1/_5$, respectively. The physical significance of this observation is the mode of transport for symmetric terminals forces the charge to redistribute equivalently across the entire flux period, consistent with what one might predict. There is not a uniform charge distribution at the Fermi crossing for M3S AC, unlike its corresponding isolated network and the M4S AD case described earlier (Fig. 9(d)), there is not a uniform charge distribution in the network for the M3S AC structure's crossing, unlike its corresponding isolated network. This is due to its Fermi crossing being between orbitals of the same type (weaker to stronger bonding orbital). In other words, for a uniform charge distribution to exist at some finite flux value within the flux period for a two-terminal network, there must be a Fermi level crossing between bonding and anti-bonding orbitals, regardless of terminal arrangement. Additionally, we can deduce that symmetric terminal arrangements do not in general indicate a symmetrical charge distribution at the center common path, but instead lead to an average uniform charge distribution between all bonds within a single flux period.

The significance of a Fermi level crossing is bolstered by another observable phenomenon related to the transmission within a given network. By examining the transmission of structures containing Fermi crossings (M3S and M4S), shown in Figs. 2 and 4, respectively, it is clear the transmission probability being driven to zero (excluding zero flux and the zone boundary) is simply the manifestation of a crossing itself. Thus, the reflected wave's magnitude is always unity in this region. This strong pull-down of the transmission to zero is similar to having a simple two-terminal AB ring with a narrowed flux period whose zone boundary is now at the Fermi level crossing. By being able to identify Fermi level crossings by observing the transmission in coupled AB ring networks, one can additionally determine when the center common path has a large portion of the total charge stored within it in the case of bonding to bonding orbital crossings, or when there is likely to be a uniform charge distribution throughout all bonds in the network for bonding to anti-bonding orbital crossings.

V. CONCLUSIONS

We examine the coupled AB rings from a purely one-dimensional point of view. In any quantum network for guided electron partial waves, there cannot be an infinite number of atoms in the network. Instead, there exist several different classes of the smallest building blocks. When each of these smallest structures is magnified properly, an identical transmission behavior will be preserved for each class. This is in a reverse trend with respect to classical microwave waveguides as far as the division of length is concerned. The finiteness for the value of M, the total number of atoms in the one-dimensional network, is the same requirement as that on the finiteness of length in microwave waveguides. While small atomic-sized AB rings can exist in pure one-dimensional form, larger 1D rings can be embedded in a mesoscopic ring of small cross section and are thus experimentally observable. For two coupled AB rings, we showed that scaling relations exist, which connect the smallest rings to larger sized rings with an identical electron transmission if the size is scaled-up any odd number of times, within the coherence length limit. The classification is determined by the parameters (l,m,n), where $l=m$ for two identical rings and $M=l+n$ is the total number of atoms. Since M is one of the classification parameters, mesoscopic rings cannot be treated as a continuum. The scaling relations presented suggest that one only needs to investigate the electron transport based on the smallest atomic-sized structures.

When the two coupled AB rings are fitted with two terminals, the bond-charge stored at the center common path is further redistributed as compared to the situation of two isolated coupled rings. In general, at zero applied flux, charge flows to the outer loop to strengthen the anti-bonding orbital, or weaken the bonding orbital, depending on where the Fermi level is. Therefore, the space-charge capacitance of the coupled rings is also continuously varied with respect to the applied flux. There is now an asymmetry of the charge storage in the common path that is correlated with the asymmetry of the two partial waves passing through the two arms between the input and output terminals. This asymmetry is flux-controllable, therefore, the electron transport can be tuned between the two arms for a given network. The net current passing through the common path is always zero. The presence or depletion of charge in the common path, paired with the ability to modulate between both states, has potential applications in nanoelectronics such as a quantum capacitor or memory storage element. We have shown the few fundamental modes that exist for the coupled electron waveguides based on 1D structures. Therefore, experimentally, we expect a dominant

mode can be observed from mesoscopic-sized coupled AB rings similar to the verification of a simple two-terminal AB ring in Ref. 7.

Finally, there is a paradox of electron transport through a quantum network. When two AB rings are coupled, the electron wave function is spread out over a larger region. However, this delocalization of the electron wave is at the expense of an increase of two more scattering centers created at the two ends of the common path. Thus, the incoming electron from the input terminal will suffer more scattering events compared to when the center common path is removed. The electron wave is then decomposed into more partial waves every time a scattering event occurs. More scattering centers lead to more backscattering and hence to the Anderson localization for the electron transport.[32] Therefore, at zero applied flux, the forward transmission will suffer generally as compared to the situation when the center common path is absent. The applied fluxes can reverse the localization trend (as in M4S and M4D cases where the bond-charge decreases) or increase the localization (as in M3S and M3D where the bond-charge increases) by being able to tune the two partial waves at the output terminal to be in or out of phase. We have shown even and odd coupled rings store the bond-charge in an opposite trend with respect to the increase of the applied flux. Thus, the ideal indicator is to observe the bond-charge at the center common path. If the common path has more than a uniform share of bond-charge, the electron wave is more localized than before and by the paradox theory stated earlier, the electron transport to the output terminal will improve. On the other hand, if the bond-charge is reduced to less than a uniform share, the electron wave is more delocalized than before and hence, the Anderson localization effect prevails and the favorable forward transmission will be reduced to a smaller flux range.

[1]A. Tonomura, N. Osakabe, T. Matsuda, T. Kawasaki, and J. Endo, Phys. Rev. Lett. **56**, 792 (1986).
[2]S. Washburn and R. A. Webb, Adv. Phys. **35**, 375 (1986).
[3]H. Ajiki and T. Ando, Physica B **201**, 349 (1994).
[4]A. Tonomura, Proc. Jpn. Acad., Ser. B: Phys. Biol. Sci. **82**, 45 (2006).
[5]R. Jackiw, A. I. Milstein, S. Y. Pi, and I. S. Terekhov, Phys. Rev. B **80**, 033413 (2009).
[6]X. C. Xie and S. D. Sarma, Phys. Rev. B **36**, 9326 (1987).
[7]R. A. Webb, S. Washburn, C. P. Umbach, and R. B. Laibowitz, Phys. Rev. Lett. **54**, 2696 (1985).
[8]N. Byers and C. N. Yang, Phys. Rev. Lett. **7**, 46 (1961).
[9]H. van Houten and C. W. J. Beenakker, Phys. Today **49**(7), 22–27 (1996).
[10]C. W. J. Beenakker and H. van Houten, in *Solid State Physics*, edited by Henry Ehrenreich and David Turnbull (Academic, San Diego, 1991), Vol. 44, pp. 1–228.
[11]B. J. van Wees, H. van Houten, C. W. J. Beenakker, J. G. Williamson, L. P. Kouwenhoven, D. van der Marel, and C. T. Foxon, Phys. Rev. Lett. **60**, 848 (1988).
[12]M. A. Topinka, B. J. LeRoy, R. M. Westervelt, S. E. J. Shaw, R. Fleischmann, E. J. Heller, K. D. Maranowski, and A. C. Gossard, Nature **410**, 183 (2001).
[13]M. P. Jura, M. A. Topinka, M. Grobis, L. N. Pfeiffer, K. W. West, and D. Goldhaber-Gordon, Phys. Rev. B **80**, 041303 (2009).
[14]P. Havu, M. J. Puska, R. M. Nieminen, and V. Havu, Phys. Rev. B **70**, 233308 (2004).
[15]T. Itoh, N. Sano, and A. Yoshii, Phys. Rev. B **45**, 14131 (1992).
[16]T. Hatano, T. Kubo, Y. Tokura, S. Amaha, S. Teraoka, and S. Tarucha, Phys. Rev. Lett. **106**, 076801 (2011).
[17]S. Russo, J. B. Oostinga, D. Wehenkel, H. B. Heersche, S. S. Sobhani, L. M. K. Vandersypen, and A. Morpurgo, Phys. Rev. B **77**, 085413 (2008).
[18]C. H. Wu and G. Mahler, Phys. Rev. B **43**, 5012 (1991).
[19]T. Chwiej and B. Szafran, Phys. Rev. B **78**, 245306 (2008).
[20]D. Awschalom, M. Flatte, and N. Samarth, *Spintronics* (Scientific American, 2002).
[21]C. A. Cain and C. H. Wu, J. Appl. Phys. **110**, 054315 (2011).
[22]C. H. Wu and D. Ramamurthy, Phys. Rev. B **65**, 075313 (2002).
[23]D. Ramamurthy and C. H. Wu, Phys. Rev. B **66**, 115307 (2002).
[24]L. Tran, M.S. thesis, Missouri University of Science and Technology, 2006.
[25]S. Alexander, Phys. Rev. B **27**, 1541 (1983).
[26]R. Landauer, Philos. Mag. **21**, 863 (1970).
[27]R. Landauer and M. Büttiker, Phys. Rev. Lett. **54**, 2049 (1985).
[28]M. Büttiker, Y. Imry, and R. Landauer, Phys. Lett. A **96**, 365 (1983).
[29]M. Büttiker, Y. Imry, and M. Azbel, Phys. Rev. A **30**, 1982 (1984).
[30]M. Büttiker, Y. Imry, R. Landauer, and S. Pinhas, Phys. Rev. B **31**, 6207 (1985).
[31]M. Büttiker, "Symmetry of electrical conduction," IBM J. Res. Dev. **32**(3), 317 (1988).
[32]P. W. Anderson, D. J. Thouless, E. Abrahams, and D. S. Fischer, Phys. Rev. B **22**, 3519 (1980).